Chapter 7
Theory of Transient Infinite Elements for Simulating Pore-Fluid Flow and Heat Transfer in Porous Media of Infinite Domains

Pore-fluid flow and heat transfer in fluid-saturated porous media of infinite domains are important phenomena in many scientific and engineering fields. For example, in the field of exploration geoscience, pore-fluid flow and heat transfer from the interior of the Earth to the surface of the Earth are two important physical processes to control ore body formation and mineralization within the upper crust of the Earth. Owing to the increasing demand of natural minerals and the possible exhaustion of existing mineral resources in the foreseeable future, there has been an ever-increasing interest in the study of key controlling processes associated with ore body formation and mineralization within the upper crust of the Earth (Phillips 1991; Yeh and Tripathi 1991; Nield and Bejan 1992; Steefel and Lasaga 1994; Raffensperger and Garven 1995; Schafer et al. 1998a, b; Xu et al. 1999; Schaubs and Zhao 2002; Ord et al. 2002; Gow et al. 2002; Zhao et al. 1997–2008). In the field of environmental engineering, carbon dioxide gas sequestration in the deep Earth is becoming a potential way to reduce the greenhouse effect. Even in our daily lives, pore-fluid flow through fluid-saturated porous soils can be encountered almost everywhere. Although pore-fluid flow and heat transfer processes in fluid-saturated porous media are often coupled together, these two processes will be considered separately in this chapter, so as to facilitate the establishment of the fundamental theory of transient infinite elements for simulating pore-fluid flow and heat transfer problems in fluid-saturated porous media of infinite domains.

In numerical simulations of infinite domains, a primitive and most simple method, in which the infinite domain was approximately truncated as a large enough finite domain, was widely used at the early stage of the finite element analysis. The major disadvantages in using this primitive method are as follows: (1) the numerical simulation for a sufficiently large domain leads to computer CPU costs and storage penalties; (2) the boundary conditions of a problem at infinity cannot be rigorously satisfied. For instance, stresses and displacements approaching zero at infinity for a static problem and the wave radiation condition in the far field for a dynamic problem are violated in the numerical analysis; (3) stretching a fixed number of finite elements to model a vast domain can result in a severe loss of solution accuracy for static problems and spurious solutions for dynamic problems due to the element size requirement for appropriately simulating dynamic problems; (4) for transient

C. Zhao, *Dynamic and Transient Infinite Elements*, Advances in Geophysical and Environmental Mechanics and Mathematics, DOI 10.1007/978-3-642-00846-7_7,

pore-fluid flow and heat transfer problems, use of artificially truncated boundaries can cause unexpected numerical reflections back into the near field, where the solutions are usually of great interest to the analyst, of a system.

For the simulation of many pore-fluid flow and heat transfer problems in scientific and engineering fields, their computational domains can be treated as either homogeneous isotropic or homogeneous orthotropic porous media of infinite extent (Bear 1972; Freeze and Cherry 1979; Zhao and Valliappan 1993g, h). From a mathematical point of view, the two mutually alien subjects of transient pore-fluid flow and heat transfer can be treated together in this chapter, because they are described by the analogous boundary value problems. Since either a homogeneous isotropic or a homogeneous orthotropic porous medium has two orthogonal principal axes, it is possible to arrange these two principal axes to coincide with the x and y axes of a Cartesian coordinate system so that the presentation of the mathematics related to the derivation of transient infinite element formulation can be greatly simplified. One of the major advantages of considering either a homogeneous isotropic or a homogeneous orthotropic porous medium is that the property matrices of two-dimensional transient infinite elements can be evaluated either analytically or numerically. In the former case, the corresponding matrices of a transient infinite element can be expressed in closed forms (Zhao and Valliappan 1993g), whereas in the latter case, the corresponding matrices need to be computed using numerical integration (Zhao and Valliappan 1993h). Consequently, from a computational point of view, two different numerical methods are demonstrated in deriving the property matrices of two-dimensional transient infinite elements. As for a porous medium of general anisotropy, from the best knowledge of the author, the formulation of two-dimensional transient infinite elements remains unavailable so that future research is needed in this respect. The main purpose of this chapter is to summarize the fundamental theories of two-dimensional transient infinite elements for simulating transient pore-fluid flow and heat transfer problems in either fluid-saturated homogeneous isotropic or fluid-saturated homogeneous orthotropic porous media consisting of infinite domains.

7.1 Fundamental Theory of Transient Infinite Elements for Simulating Pore-Fluid Flow Problems in Fluid-Saturated Porous Media of Infinite Domains

7.1.1 Derivation of the Hydraulic Head Distribution Functions of Transient Infinite Elements

The key issue of constructing transient infinite elements for simulating pore-fluid flow problems in fluid-saturated porous media of infinite domains is to appropriately propose a hydraulic head distribution function in the infinite direction of the element. A general form of the hydraulic head distribution function for such a transient infinite element can be derived from the analytical solution of a representative problem. For this purpose, a pore-fluid flow problem, which has a unit hydraulic head at the origin of a Cartesian coordinate system in a one-dimensional fluid-saturated porous medium of infinite domain, is considered to derive the general form of the hydraulic head distribution function for such a transient infinite element. The governing equation of this one-dimensional problem in a fluid-saturated porous medium of infinite domain can be written as follows (Freeze and Cherry 1979; Zhao and Valliappan 1993g):

$$K_x \frac{\partial^2 h}{\partial x^2} = S_s \frac{\partial h}{\partial t}, \tag{7.1}$$

where K_x is the hydraulic conductivity in the x direction; h is the hydraulic head that represents energy per unit weight of pore-fluid (i.e. water); S_s is the specific storage of a saturated aquifer (i.e. porous medium) and is defined as the volume of pore-fluid released from a unit volume of the aquifer under a unit decline in hydraulic head. Since a decrease in hydraulic head implies either a decrease in pore-fluid pressure or an increase in effective stress, the pore fluid released from the aquifer under the condition of decreasing hydraulic head is mainly caused by the following two mechanisms. The first mechanism is the compression of the aquifer as a result of increasing effective stress so that it is controlled by the aquifer (i.e. porous medium) compressibility, α, while the second mechanism is the expansion of the pore fluid as a result of decreasing pore-fluid pressure so that it is controlled by the pore-fluid compressibility, β. Thus, the specific storage of a fluid-saturated aquifer can be expressed as follows (Freeze and Cherry 1979):

$$S_s = \rho_f g(\alpha + \phi\beta), \tag{7.2}$$

where ρ_f is the pore-fluid density; g is the acceleration due to gravity; ϕ is the porosity of the porous medium. Note that the specific storage (S_s) has the dimension of L^{-1}.

For constant K_x and S_s, the analytical solution for this one-dimensional pore-fluid flow problem with a unit hydraulic head at the origin of the Cartesian coordinate system can be expressed in the following form (Carslaw and Jaeger 1959; Harr 1962):

$$h(x, t) = \sqrt{\frac{S_s}{4\pi K_x t}} \exp\left(-\frac{S_s x^2}{4K_x t}\right). \tag{7.3}$$

For a typical transient infinite element shown in Fig. 7.1, the global coordinate of node 1 is x_1 and the local coordinate of this node is identical to zero. The hydraulic head at this node for a given time, t, can be expressed as:

$$h(x_1, t) = \sqrt{\frac{S_s}{4\pi K_x t}} \exp\left(-\frac{S_s x_1^2}{4K_x t}\right). \tag{7.4}$$

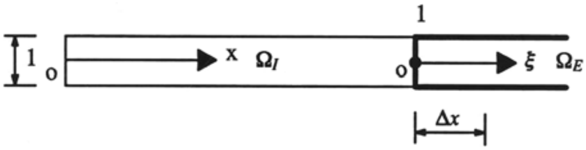

Fig. 7.1 A typical one-dimensional transient infinite element for simulating transient pore-fluid flow problems

For any point within this transient infinite element, taking $x = x_1 + \Delta x$ as an example, the hydraulic head at this point can be directly derived from Eq. (7.4):

$$h(x_1 + \Delta x, t) = h(x_{1,} t) \exp\left[-\frac{S_s(\Delta x^2 + 2x_1 \Delta x)}{4K_x t}\right]. \tag{7.5}$$

Since $\xi = \Delta x$ for this one-dimensional transient infinite element, the hydraulic head distribution function of this element can be expressed as

$$F_{hd}(\xi, t) = \exp\left[-\frac{S_s(\xi^2 + 2x_1\xi)}{4K_x t}\right]. \tag{7.6}$$

As a result, the hydraulic head field within the one-dimensional transient infinite element can be expressed using the following equation:

$$h(\xi,t) = h_1 F_{hd}(\xi,t) = h_1 N_1, \tag{7.7}$$

where h_1 is the nodal hydraulic head of the one-dimensional transient infinite element; h is the hydraulic head distribution within the infinite element; N_1 is the shape function of the one-dimensional transient infinite element. Note that for one-dimensional transient pore-fluid flow problems, the hydraulic head distribution function is identical to the shape function of the one-dimensional transient infinite element.

$$N_1 = F_{hd}(\xi, t) = \exp\left[-\frac{S_s(\xi^2 + 2x_1\xi)}{4K_x t}\right]. \tag{7.8}$$

The first derivative of the shape function with respect to ξ is

$$\frac{\partial N_1}{\partial \xi} = -\frac{S_s(\xi + x_1)}{2K_x t} \exp\left[-\frac{S_s(\xi^2 + 2x_1\xi)}{4K_x t}\right]. \tag{7.9}$$

Using the finite element method (Zienkiewicz 1977; Rao 1989) and the condition of $dx = d\xi$, the property matrices of the one-dimensional transient infinite element can be expressed as

$$G_{11} = \int_0^{\infty} \left(\frac{K_x}{S_s} \frac{\partial N_1}{\partial \xi} \frac{\partial N_1}{\partial \xi} \right) d\xi, \tag{7.10}$$

$$R_{11} = \int_0^{\infty} (N_1 N_1)\, d\xi. \tag{7.11}$$

Substituting Eqs. (7.8) and (7.9) into Eqs. (7.10) and (7.11) yields

$$G_{11} = \frac{S_s}{4K_x t^2} \int_0^{\infty} \left\{ (\xi + x_1)^2 \exp\left[-\frac{S_s(\xi^2 + 2x_1\xi)}{2K_x t} \right] \right\} d\xi, \tag{7.12}$$

$$R_{11} = \int_0^{\infty} \exp\left[-\frac{S_s(\xi^2 + 2x_1\xi)}{2K_x t} \right] d\xi. \tag{7.13}$$

To evaluate Eqs. (7.12) and (7.13), the following integrals have been encountered:

$$I_1 = \int_0^{\infty} \exp\left(-x^2\right) dx = \frac{\sqrt{\pi}}{2}, \tag{7.14}$$

$$I_2 = \int_0^{\infty} x^2 \exp\left(-x^2\right) dx = \frac{\sqrt{\pi}}{4}, \tag{7.15}$$

$$I_3 = \int_a^{\infty} \exp\left(-x^2\right) dx = \frac{\sqrt{\pi}}{2} - \sum_{n=0}^{\infty} \frac{(-1)^n}{n!} \frac{1}{2n+1} a^{2n+1}, \tag{7.16}$$

$$I_4 = \int_a^{\infty} x^2 \exp\left(-x^2\right) dx = \frac{\sqrt{\pi}}{4} + \frac{a}{2} e^{-a^2} - \frac{1}{2} \sum_{n=0}^{\infty} \frac{(-1)^n}{n!} \frac{1}{2n+1} a^{2n+1}. \tag{7.17}$$

Note that mathematically, the value of an integral is independent of the symbol of the integration variable used in the integral. Thus, using these integrals expressed in Eqs. (7.14), (7.15), (7.16) and (7.17), Eqs. (7.12) and (7.13), after some mathematical manipulations, can be expressed as

$$R_{11} = \sqrt{\frac{2K_x t}{S_s}} \exp\left(\frac{S_s x_1^2}{2K_x t} \right) \left[\frac{\sqrt{\pi}}{2} - \sum_{n=0}^{\infty} \left(\frac{(-1)^n}{n!} \frac{1}{2n+1} \lambda_1^{2n+1} \right) \right], \tag{7.18}$$

$$\begin{aligned} G_{11} = {} & \sqrt{\frac{K_x}{8S_s t}} \exp\left(\frac{S_s x_1^2}{2K_x t} \right) \left[\frac{\sqrt{\pi}}{2} + \lambda_1 \exp\left(-\frac{S_s x_1^2}{2K_x t} \right) \right. \\ & \left. - \sum_{n=0}^{\infty} \left(\frac{(-1)^n}{n!} \frac{1}{2n+1} \lambda_1^{2n+1} \right) \right]. \end{aligned} \tag{7.19}$$

$$\lambda_1 = x_1 \sqrt{\frac{S_s}{2K_x t}}. \tag{7.20}$$

Similarly, if the positive direction of the ξ-axis in the local coordinate system is opposite to that of the x-axis in the global coordinate system, the hydraulic head distribution function of the one-dimensional transient infinite element can be expressed as follows:

$$F_{hd}^{*}(\xi, t) = \exp\left[-\frac{S_s(\xi^2 - 2x_1\xi)}{4K_x t}\right]. \tag{7.21}$$

Consequently, the corresponding property matrices of the one-dimensional transient infinite element can be expressed using the following equations:

$$R_{11}^{*} = \sqrt{\frac{2K_x t}{S_s}} \exp\left(\frac{S_s x_1^2}{2K_x t}\right)\left[\frac{\sqrt{\pi}}{2} - \sum_{n=0}^{\infty}\left(\frac{(-1)^n}{n!}\frac{1}{2n+1}\lambda_2^{2n+1}\right)\right], \tag{7.22}$$

$$\begin{aligned} G_{11}^{*} = \sqrt{\frac{K_x}{8S_s t}} \exp\left(\frac{S_s x_1^2}{2K_x t}\right)\Bigg[\frac{\sqrt{\pi}}{2} + \lambda_2 \exp\left(-\frac{S_s x_1^2}{2K_x t}\right) \\ -\sum_{n=0}^{\infty}\left(\frac{(-1)^n}{n!}\frac{1}{2n+1}\lambda_2^{2n+1}\right)\Bigg], \end{aligned} \tag{7.23}$$

$$\lambda_2 = -x_1\sqrt{\frac{S_s}{2K_x t}}. \tag{7.24}$$

After the general form of the hydraulic head distribution function is derived for a one-dimensional transient infinite element, the same procedure can be used to derive the general form of the hydraulic head distribution function for a two-dimensional transient infinite element. If a two-dimensional pore-fluid flow problem, which has a point hydraulic head at the origin of a Cartesian coordinate system in a fluid-saturated homogeneous, orthotropic porous medium of infinite extent, is considered, then the governing equation of this problem (Freeze and Cherry 1979; Zhao and Valliappan 1993g) can be expressed as follows:

$$K_x\frac{\partial^2 h}{\partial x^2} + K_y\frac{\partial^2 h}{\partial y^2} = S_s\frac{\partial h}{\partial t}, \tag{7.25}$$

where K_x and K_y are the hydraulic conductivities in the x and y directions, which are two principal directions of the fluid-saturated homogeneous and orthotropic porous medium; h is the hydraulic head in the fluid-saturated porous medium of the infinite domain.

For constant K_x, K_y and S_s, the analytical solution for the hydraulic head of this problem (Larder and Song 1991) can be expressed as

$$h(x, y, t) = \sqrt{\frac{S_s}{4\pi K_x t}}\sqrt{\frac{S_s}{4\pi K_y t}} h_0 \exp\left(-\frac{S_s x^2}{4K_x t}\right)\exp\left(-\frac{S_s y^2}{4K_y t}\right), \tag{7.26}$$

where h_0 is the point hydraulic head at the origin of the Cartesian coordinate system.

In order to derive the hydraulic head distribution function for a two-dimensional transient infinite element, Eq. (7.21) can be straightforwardly rewritten into the form:

$$h(x, y, t) = h_0 g_1(x, t) g_2(y, t), \tag{7.27}$$

where

$$g_1(x, t) = \sqrt{\frac{S_s}{4\pi K_x t}} \exp\left(-\frac{S_s x^2}{4K_x t}\right), \tag{7.28}$$

$$g_2(y, t) = \sqrt{\frac{S_s}{4\pi K_y t}} \exp\left(-\frac{S_s y^2}{4K_y t}\right). \tag{7.29}$$

Since the orthotropy of the porous medium and the different features of pore-fluid flow are considered in the two principal directions of the porous medium, more shapes of transient infinite elements need to be considered in the course of constructing transient infinite elements for the simulation of two-dimensional transient pore-fluid flow problems in fluid-saturated porous media of infinite domains. As shown in Fig. 7.2, if the positive directions of pore-fluid flow are identical to those of the x- and y-axes, then eight categories of transient infinite elements should

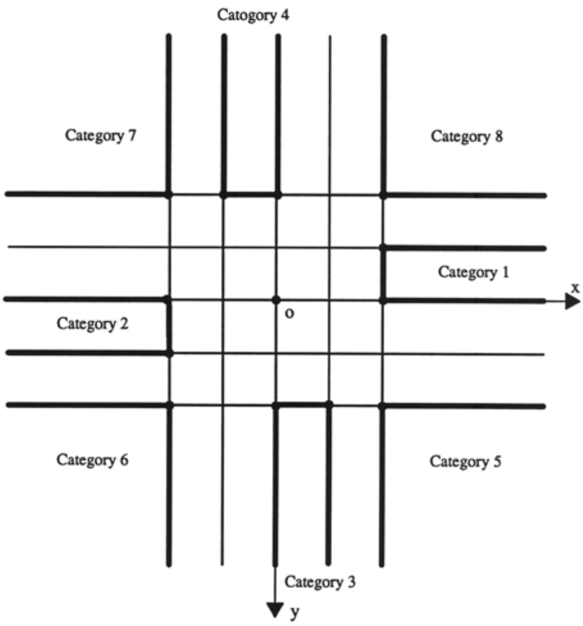

Fig. 7.2 Eight categories of two-dimensional transient infinite elements for simulating transient pore-fluid flow problems

be constructed to simulate two-dimensional transient pore-fluid flow problems in a full infinite plane. According to the feature of infinite extent, the transient infinite elements in categories one to four are called uni-infinite elements, while the transient infinite elements in categories five to eight are called bi-infinite elements. Following the same procedure as that used to derive the hydraulic head distribution function for one-dimensional transient pore-fluid flow problems, the general forms of hydraulic head distribution functions for two-dimensional transient pore-fluid flow problems in fluid-saturated porous media of infinite domains can be derived and expressed as follows:

$$F_{hd}(\xi, t) = \exp\left[-\frac{S_s(\xi^2 + 2x_1\xi)}{4K_x t}\right], \tag{7.30}$$

$$F_{hd}^*(\xi, t) = \exp\left[-\frac{S_s(\xi^2 - 2x_1\xi)}{4K_x t}\right], \tag{7.31}$$

$$F_{hd}(\eta, t) = \exp\left[-\frac{S_s(\eta^2 + 2y_1\eta)}{4K_y t}\right], \tag{7.32}$$

$$F_{hd}^*(\eta, t) = \exp\left[-\frac{S_s(\eta^2 - 2y_1\eta)}{4K_y t}\right], \tag{7.33}$$

where $F_{hd}(\xi, t)$ and $F_{hd}^*(\xi, t)$ are the hydraulic head distribution functions of two-dimensional transient infinite elements when the positive direction of the ξ axis is identical or opposite to that of the x axis; $F_{hd}(\eta, t)$ and $F_{hd}^*(\eta, t)$ are the hydraulic head distribution functions of two-dimensional transient infinite elements when the positive direction of the η axis is identical or opposite to that of the y axis, respectively; x_1 and y_1 are nodal coordinates in the global coordinate system.

7.1.2 Derivation of the Property Matrices of Two-Dimensional Transient Infinite Elements for Simulating Pore-Fluid Flow Problems

Another key issue associated with the construction of two-dimensional transient infinite elements is to derive the property matrices of the transient infinite elements in a mathematical manner. Generally, there are two ways that can be used to derive the property matrices of two-dimensional transient infinite elements. The first way is to use more different kinds of parent infinite elements, which have different shapes, in the process of deriving the property matrices of the transient infinite elements, while the second way is to use only two kinds of mapped parent infinite elements in the process of deriving the property matrices of two-dimensional transient infinite elements. Owing to this significant difference, the property matrices derived using the first way can be expressed in closed forms, but the property matrices derived using the second way need to be evaluated numerically. In this section, the first way is used to derive the property matrices of two-dimensional transient infinite elements that can be employed to simulate two-dimensional transient pore-fluid flow problems in fluid-saturated porous media of infinite domains. To avoid unnecessary repeats, the second way will be adopted in the next section to derive the property matrices of two-dimensional transient infinite elements, which can be used to simulate two-dimensional heat transfer problems in fluid-saturated porous media of infinite domains.

Since the governing equation is of the same mathematical form for both a finite element and a transient infinite element, the conventional finite element method (Zienkiewicz 1997; Rao 1989) can be used to derive the property matrices of transient infinite elements. Using the Galerkin weighted residual method, Eq. (7.25) can be discretized into a set of algebraic equations as follows:

$$[G]\{h\} + [R]\left\{\frac{\partial h}{\partial t}\right\} = \{f\}, \tag{7.34}$$

where $\{h\}$ is the global nodal hydraulic head vector of the system; $\{f\}$ is the global nodal "load" vector of the system; $[G]$ and $[R]$ are the global property matrices of the system and their element property matrices can be expressed as

$$[G_e] = \iint_A \left(\frac{K_x}{S_s}\frac{\partial[N]^T}{\partial x}\frac{\partial[N]}{\partial x} + \frac{K_y}{S_s}\frac{\partial[N]^T}{\partial y}\frac{\partial[N]}{\partial y}\right) dA, \tag{7.35}$$

$$[R_e] = \iint_A \left([N]^T[N]\right) dA, \tag{7.36}$$

where $[N]$ is the (hydraulic head) shape function matrix of either a finite element or a transient infinite element; $[N]^T$ is the transpose of $[N]$; A is the area of the corresponding element.

7.1.2.1 The First Category of Two-Dimensional Transient Infinite Elements

As shown in Fig. 7.3(A), the shape function matrix of this category of two-dimensional transient infinite elements can be written as follows:

$$[N] = [N_1 \quad N_2] \tag{7.37}$$

where N_1 and N_2 are the shape functions for nodes 1 and 2 of the element, respectively.

$$N_1 = F_{hd}(\xi,t)\frac{1-\eta}{2}, \tag{7.38}$$

$$N_2 = F_{hd}(\xi,t)\frac{1+\eta}{2}. \tag{7.39}$$

Fig. 7.3 Four categories of two-dimensional transient uni-infinite elements

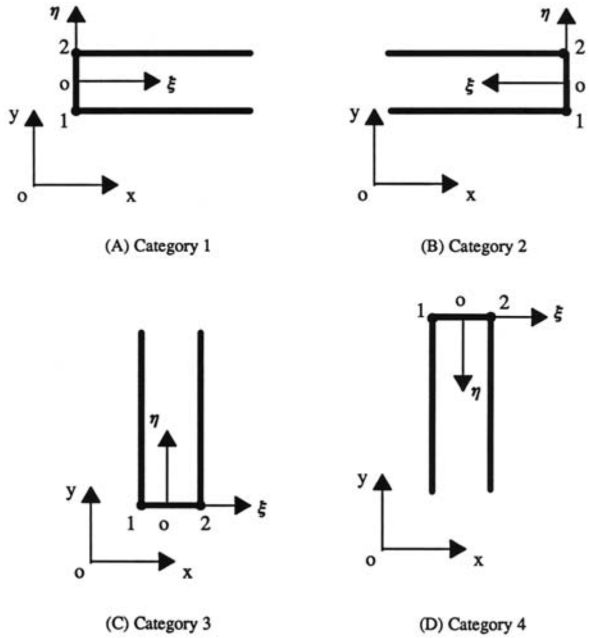

It is noted that for this category of two-dimensional transient infinite elements, the following relationship exists between the local coordinate system and the global one.

$$dx = d\xi, \tag{7.40}$$

$$dy = \frac{1}{2}(y_2 - y_1)d\eta. \tag{7.41}$$

Substituting Eqs. (7.37), (7.38), (7.39), (7.40) and (7.41) into Eqs. (7.35) and (7.36) yields the property matrices of the first category of two-dimensional transient infinite elements as follows:

$$[G_e]_1 = \int_0^{\infty} \int_{-1}^{1} \left(\frac{K_x}{S_s} \frac{\partial [N]^T}{\partial \xi} \frac{\partial [N]}{\partial \xi} + \frac{4K_y}{S_s (y_2 - y_1)^2} \frac{\partial [N]^T}{\partial \eta} \frac{\partial [N]}{\partial \eta} \right) \frac{y_2 - y_1}{2} d\eta d\xi, \tag{7.42}$$

$$[R_e]_1 = \int_0^{\infty} \int_{-1}^{1} \left([N]^T [N] \right) \frac{y_2 - y_1}{2} d\eta d\xi \tag{7.43}$$

After Eqs. (7.42) and (7.43) are integrated analytically, the resulting property matrices of the first category of two-dimensional transient infinite elements can be expressed in the following forms:

$$[G_e]_1 = \frac{K_x(y_2 - y_1)}{3S_s} G_{11}(x_1, t) \begin{bmatrix} 1 & 0.5 \\ 0.5 & 1 \end{bmatrix} + \frac{K_y}{S_s(y_2 - y_1)} R_{11}(x_1, t) \begin{bmatrix} 1 & -1 \\ -1 & 1 \end{bmatrix}, \tag{7.44}$$

$$[R_e]_1 = \frac{y_2 - y_1}{3} R_{11}(x_1, t) \begin{bmatrix} 1 & 0.5 \\ 0.5 & 1 \end{bmatrix}, \tag{7.45}$$

where $R_{11}(x_1, t)$ and $G_{11}(x_1, t)$ are defined below:

$$R_{11}(x_1, t) = \sqrt{\frac{2K_x t}{S_s}} \exp\left(\lambda_1^2\right) \left[\frac{\sqrt{\pi}}{2} - \sum_{n=0}^{\infty} \left(\frac{(-1)^n}{n!} \frac{1}{2n+1} \lambda_1^{2n+1} \right) \right], \tag{7.46}$$

$$G_{11}(x_1, t) = \sqrt{\frac{S_s}{8K_x t}} \exp\left(\lambda_1^2\right) \left[\frac{\sqrt{\pi}}{2} + \lambda_1 \exp\left(-\lambda_1^2\right) - \sum_{n=0}^{\infty} \left(\frac{(-1)^n}{n!} \frac{1}{2n+1} \lambda_1^{2n+1} \right) \right], \tag{7.47}$$

where

$$\lambda_1 = x_1 \sqrt{\frac{S_s}{2K_x t}}. \tag{7.48}$$

7.1.2.2 The Second Category of Two-Dimensional Transient Infinite Elements

Figure 7.3(B) shows the second category of two-dimensional transient infinite elements, the main characteristic of which is that the positive direction of the x axis is opposite to that of the ξ axis. The shape function matrix of this category of two-dimensional transient infinite elements can be expressed as follows:

$$[N] = [N_1 \quad N_2], \tag{7.49}$$

where N_1 and N_2 are the shape functions for nodes 1 and 2 of the element, respectively.

$$N_1 = F_{hd}^*(\xi, t) \frac{1 - \eta}{2}, \tag{7.50}$$

$$N_2 = F_{hd}^*(\xi, t) \frac{1 + \eta}{2}. \tag{7.51}$$

Following the similar procedure to that used above, the property matrices of the second category of two-dimensional transient infinite elements can be derived as follows:

$$[G_e]_2 = \frac{K_x(y_2 - y_1)}{3S_s} G_{11}^*(x_1,t) \begin{bmatrix} 1 & 0.5 \\ 0.5 & 1 \end{bmatrix} + \frac{K_y}{S_s(y_2 - y_1)} R_{11}^*(x_1,t) \begin{bmatrix} 1 & -1 \\ -1 & 1 \end{bmatrix}, \tag{7.52}$$

$$[R_e]_2 = \frac{y_2 - y_1}{3} R_{11}^*(x_1,t) \begin{bmatrix} 1 & 0.5 \\ 0.5 & 1 \end{bmatrix}, \tag{7.53}$$

where $R_{11}^*(x_1,t)$ and $G_{11}^*(x_1,t)$ are defined below:

$$R_{11}^*(x_1,t) = \sqrt{\frac{2K_x t}{S_s}} \exp\left(\lambda_2^2\right) \left[\frac{\sqrt{\pi}}{2} - \sum_{n=0}^{\infty} \left(\frac{(-1)^n}{n!} \frac{1}{2n+1} \lambda_2^{2n+1}\right)\right], \tag{7.54}$$

$$\begin{aligned} G_{11}^*(x_1,t) = \sqrt{\frac{S_s}{8K_x t}} \exp\left(\lambda_2^2\right) \left[\frac{\sqrt{\pi}}{2} + \lambda_2 \exp\left(-\lambda_2^2\right)\right. \\ \left. - \sum_{n=0}^{\infty} \left(\frac{(-1)^n}{n!}\right) \frac{1}{2n+1} \lambda_2^{2n+1}\right], \end{aligned} \tag{7.55}$$

where

$$\lambda_2 = -x_1 \sqrt{\frac{S_s}{2K_x t}} \tag{7.56}$$

7.1.2.3 The Third Category of Two-Dimensional Transient Infinite Elements

The fundamental characteristic of the third category of two-dimensional transient infinite elements is that their sizes extend to infinity in the η direction, instead of the ξ direction. In order to simulate the vertical component of the pore-fluid flow, it is assumed that the η axis is parallel to the y axis. As shown in Fig. 7.3(C), the shape function matrix of this category of two-dimensional transient infinite elements can be written as follows:

$$[N] = [N_1 \quad N_2], \tag{7.57}$$

where N_1 and N_2 are the shape functions for nodes 1 and 2 of the infinite element, respectively.

$$N_1 = F_{hd}(\eta,t) \frac{1-\xi}{2}, \tag{7.58}$$

$$N_2 = F_{hd}(\eta,t) \frac{1+\xi}{2}. \tag{7.59}$$

Using the similar procedure to that used above, the property matrices of the third category of two-dimensional transient infinite elements can be derived as follows:

$$[G_e]_3 = \frac{K_x}{S_s(x_2 - x_1)} R_{11}(y_1, t) \begin{bmatrix} 1 & -1 \\ -1 & 1 \end{bmatrix} + \frac{K_y(x_2 - x_1)}{3S_s} G_{11}(y_1, t) \begin{bmatrix} 1 & 0.5 \\ 0.5 & 1 \end{bmatrix}, \tag{7.60}$$

$$[R_e]_3 = \frac{x_2 - x_1}{3} R_{11}(y_1, t) \begin{bmatrix} 1 & 0.5 \\ 0.5 & 1 \end{bmatrix}, \tag{7.61}$$

where $R_{11}(y_1, t)$ and $G_{11}(y_1, t)$ are defined below:

$$R_{11}(y_1, t) = \sqrt{\frac{2K_y t}{S_s}} \exp\left(\lambda_3^2\right) \left[\frac{\sqrt{\pi}}{2} - \sum_{n=0}^{\infty} \left(\frac{(-1)^n}{n!} \frac{1}{2n+1} \lambda_3^{2n+1} \right) \right], \tag{7.62}$$

$$\begin{aligned} G_{11}(y_1, t) = \sqrt{\frac{S_s}{8K_y t}} \exp\left(\lambda_3^2\right) \left[\frac{\sqrt{\pi}}{2} + \lambda_3 \exp\left(-\lambda_3^2\right) \right. \\ \left. - \sum_{n=0}^{\infty} \left(\frac{(-1)^n}{n!} \frac{1}{2n+1} \lambda_3^{2n+1} \right) \right], \end{aligned} \tag{7.63}$$

where

$$\lambda_3 = y_1 \sqrt{\frac{S_s}{2K_y t}}. \tag{7.64}$$

7.1.2.4 The Fourth Category of Two-Dimensional Transient Infinite Elements

The basic characteristic of the fourth category of two-dimensional transient infinite elements is that the positive direction of the η direction is opposite to that of the y-axis. As shown in Fig. 7.3(D), the shape function matrix of this category of two-dimensional transient infinite elements can be expressed as follows:

$$[N] = [N_1 \quad N_2], \tag{7.65}$$

where N_1 and N_2 are the shape functions for nodes 1 and 2 of the infinite element, respectively:

$$N_1 = F_{hd}^*(\eta, t) \frac{1 - \xi}{2}, \tag{7.66}$$

$$N_2 = F_{hd}^*(\eta, t) \frac{1 + \xi}{2}. \tag{7.67}$$

Similarly, the property matrices of the fourth category of two-dimensional transient infinite elements can be derived as follows:

$$[G_e]_4 = \frac{K_x}{S_s(x_2 - x_1)} R_{11}^*(y_1, t) \begin{bmatrix} 1 & -1 \\ -1 & 1 \end{bmatrix} + \frac{K_y(x_2 - x_1)}{3S_s} G_{11}^*(y_1, t) \begin{bmatrix} 1 & 0.5 \\ 0.5 & 1 \end{bmatrix}, \tag{7.68}$$

$$[R_e]_4 = \frac{x_2 - x_1}{3} R_{11}^*(y_1,t) \begin{bmatrix} 1 & 0.5 \\ 0.5 & 1 \end{bmatrix}, \tag{7.69}$$

where $R_{11}^*(y_1, t)$ and $G_{11}^*(y_1, t)$ are defined below:

$$R_{11}^*(y_1,t) = \sqrt{\frac{2K_y t}{S_s}} \exp\left(\lambda_4^2\right) \left[\frac{\sqrt{\pi}}{2} - \sum_{n=0}^{\infty} \left(\frac{(-1)^n}{n!} \frac{1}{2n+1} \lambda_4^{2n+1} \right) \right], \tag{7.70}$$

$$\begin{aligned} G_{11}^*(y_1, t) = \sqrt{\frac{S_s}{8K_y t}} \exp\left(\lambda_4^2\right) \left[\frac{\sqrt{\pi}}{2} + \lambda_4 \exp\left(-\lambda_4^2\right) \right. \\ \left. - \sum_{n=0}^{\infty} \left(\frac{(-1)^n}{n!} \frac{1}{2n+1} \lambda_4^{2n+1} \right) \right], \end{aligned} \tag{7.71}$$

where

$$\lambda_4 = -y_1 \sqrt{\frac{S_s}{2K_y t}}. \tag{7.72}$$

7.1.2.5 Two-Dimensional Transient Bi-infinite Elements

The fifth to eighth categories of two-dimensional transient infinite elements are called bi-infinite elements due to their infinite extension in both the ξ and the η directions. Following the same procedures as those used in the previous subsections, the property matrices of two-dimensional transient bi-infinite elements can be derived and expressed below.

For the fifth category of two-dimensional transient infinite elements shown in Fig. 7.4(A), the corresponding property matrices are as follows:

$$[G_e]_5 = \frac{K_x}{S_s} G_{11}(x_1, t) R_{11}(y_1, t) + \frac{K_y}{S_s} R_{11}(x_1, t) G_{11}(y_1, t), \tag{7.73}$$

$$[R_e]_5 = R_{11}(x_1, t) R_{11}(y_1, t). \tag{7.74}$$

For the sixth category of two-dimensional transient infinite elements shown in Fig. 7.4(B), the corresponding property matrices can be expressed as follows:

$$[G_e]_6 = \frac{K_x}{S_s} G_{11}^*(x_1, t) R_{11}(y_1, t) + \frac{K_y}{S_s} R_{11}^*(x_1, t) G_{11}(y_1, t), \tag{7.75}$$

$$[R_e]_6 = R_{11}^*(x_1, t) R_{11}(y_1, t). \tag{7.76}$$

Fig. 7.4 Four categories of two-dimensional transient bi-infinite elements

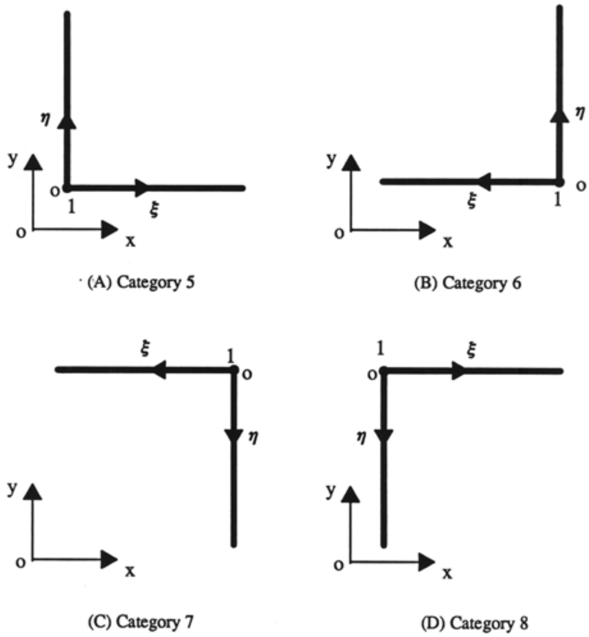

For the seventh category of two-dimensional transient infinite elements shown in Fig. 7.4(C), the corresponding property matrices can be written as follows:

$$[G_e]_7 = \frac{K_x}{S_s} G^*_{11}(x_1, t) R^*_{11}(y_1, t) + \frac{K_y}{S_s} R^*_{11}(x_1, t) G^*_{11}(y_1, t), \tag{7.77}$$

$$[R_e]_7 = R^*_{11}(x_1, t) R^*_{11}(y_1, t). \tag{7.78}$$

Finally, for the eighth category of two-dimensional transient infinite elements shown in Fig. 7.4(D), the corresponding property matrices can be expressed as follows:

$$[G_e]_8 = \frac{K_x}{S_s} G_{11}(x_1, t) R^*_{11}(y_1, t) + \frac{K_y}{S_s} R_{11}(x_1, t) G^*_{11}(y_1, t), \tag{7.79}$$

$$[R_e]_8 = R_{11}(x_1, t) R^*_{11}(y_1, t). \tag{7.80}$$

Up to now, closed-form solutions have been derived for all property matrices of two-dimensional transient infinite elements, which can be used to simulate the far fields of transient pore-fluid flow problems in two-dimensional fluid-saturated porous media of infinite domains. Since the series involved in the property matrices of two-dimensional transient infinite elements converges for all real numbers, the computation of these property matrices can be easily carried out using any computers. This is the main advantage in deriving closed-form solutions for all property matrices of two-dimensional transient infinite elements of eight different shapes.

7.2 Fundamental Theory of Transient Infinite Elements for Simulating Heat Transfer Problems in Fluid-Saturated Porous Media of Infinite Domains

7.2.1 Derivation of the Heat Transfer Functions of Transient Infinite Elements

Like constructing transient infinite elements for simulating pore-fluid flow problems, the key issue of constructing transient infinite elements for simulating heat transfer problems in fluid-saturated porous media of infinite domains is to appropriately choose a heat transfer function in the infinite direction of the element. The general form of the heat transfer function for such a transient infinite element can be derived from the analytical solution of a representative one-dimensional heat transfer problem in an infinite domain. For this particular purpose, a heat advection–conduction problem, which has a given temperature at the origin of a Cartesian coordinate system in a one-dimensional fluid-saturated porous medium of an infinite domain, is considered to derive the general form of the heat transfer function. If heat equilibrium is attained between the pore fluid and the solid matrix, the governing equation of this one-dimensional heat transfer problem in a fluid-saturated porous medium of an infinite domain (Nield and Bejan 1992) can be written as follows:

$$[\phi c_{pf}\rho_f + (1-\phi)c_{ps}\rho_s]\frac{\partial T}{\partial t} + c_{pf}\rho_f V_x \frac{\partial T}{\partial x} = [\phi\lambda_{xf} + (1-\phi)\lambda_{xs}]\frac{\partial^2 T}{\partial x^2}, \quad (7.81)$$

where c_{pf} and c_{ps} are the specific heats for the pore-fluid and solid matrix; ρ_f and ρ_s are the densities of the pore-fluid and solid matrix; λ_{xf} and λ_{xs} are the thermal conductivities of the pore-fluid and solid matrix, respectively; ϕ is the porosity of the porous medium; V_x is the Darcy velocity in the x direction; T is the temperature of the porous medium.

It is obvious that Eq. (7.81) can be rewritten into the following form:

$$(c_p\rho)_m \frac{\partial T}{\partial t} + \alpha(c_p\rho)_m V_x \frac{\partial T}{\partial x} = \lambda_x^m \frac{\partial^2 T}{\partial x^2}, \quad (7.82)$$

where

$$\lambda_x^m = \phi\lambda_{xf} + (1-\phi)\lambda_{xs}, \quad (7.83)$$

$$(c_p\rho)_m = \phi c_{pf}\rho_f + (1-\phi)c_{ps}\rho_s, \quad (7.84)$$

$$\alpha = \frac{c_{pf}\rho_f}{\phi c_{pf}\rho_f + (1-\phi)c_{ps}\rho_s}. \tag{7.85}$$

If the coefficients in front of the derivatives of Eq. (7.82) are constant, the analytical solution for this partial differential equation with a unit constant temperature at the origin of the global coordinate system can be expressed as follows (Carslaw and Jaeger 1959):

$$T(x,t) = \sqrt{\frac{(c_p\rho)_m}{4\pi\lambda_x^m t}} \exp\left[-\frac{(c_p\rho)_m(x-\alpha V_x t)^2}{4\lambda_x^m t}\right]. \tag{7.86}$$

For a transient infinite element shown in Fig. 7.5, the global coordinate of node 1 is x_1, while the local coordinate of this node is zero. To express the relationship between the positive direction of the x axis and that of the ξ axis, node 2 is defined for this transient infinite element. It is assumed that the global coordinate of node 2 is x_2 and that the local coordinate is 1. The temperature of node 1 at a given time, t, can be expressed as follows:

$$T(x_1,t) = \sqrt{\frac{(c_p\rho)_m}{4\pi\lambda_x^m t}} \exp\left[-\frac{(c_p\rho)_m(x_1-\alpha V_x t)^2}{4\lambda_x^m t}\right]. \tag{7.87}$$

For any point within this transient infinite element, taking $x = x_1 + \Delta x$ as an example, the corresponding temperature at this point can be written below:

$$T(x_1+\Delta x,t) = T(x_1,t)\exp\left\{-\frac{(c_p\rho)_m[\Delta x^2 + 2\Delta x(x_1-\alpha V_x t)]}{4\lambda_x^m t}\right\}. \tag{7.88}$$

Because $\xi = \Delta x$ for this one-dimensional transient infinite element, the heat transfer function of this transient infinite element can be expressed as follows:

$$F_{ht}(\xi,t) = \exp\left\{-\frac{(c_p\rho)_m[\xi^2 + 2\xi(x_1-\alpha V_x t)]}{4\lambda_x^m t}\right\}. \tag{7.89}$$

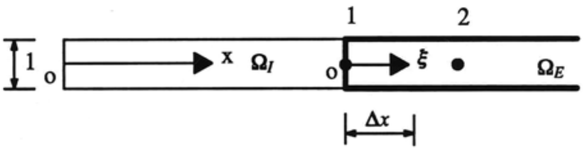

Fig. 7.5 A one-dimensional mapped transient infinite element for simulating transient heat transfer problems

7.2.2 Derivation of the Property Matrices of Two-Dimensional Transient Infinite Elements for Simulating Heat Transfer Problems

Following the same procedures as those used in the previous section, the property matrices of the transient two-dimensional infinite elements for simulating heat transfer problems can be derived in a mathematical manner. Supposing the principal heat conduction directions of an orthotropic porous medium are parallel to the x and y axes in a global Cartesian coordinate system, the governing equation of a heat transfer problem in a uniform pore-fluid flow field (Nield and Bejan 1992; Zhao and Valliappan 1993h) can be expressed as follows:

$$(c_p\rho)_m\frac{\partial T}{\partial t}+\alpha(c_p\rho)_m V_x\frac{\partial T}{\partial x}+\alpha(c_p\rho)_m V_y\frac{\partial T}{\partial y}=\lambda_x^m\frac{\partial^2 T}{\partial x^2}+\lambda_y^m\frac{\partial^2 T}{\partial y^2}, \tag{7.90}$$

where

$$\lambda_x^m=\phi\lambda_{xf}+(1-\phi)\lambda_{xs}, \tag{7.91}$$

$$\lambda_y^m=\phi\lambda_{yf}+(1-\phi)\lambda_{ys}, \tag{7.92}$$

$$(c_p\rho)_m=\phi c_{pf}\rho_f+(1-\phi)c_{ps}\rho_s, \tag{7.93}$$

$$\alpha=\frac{c_{pf}\rho_f}{\phi c_{pf}\rho_f+(1-\phi)c_{ps}\rho_s}, \tag{7.94}$$

where c_{pf} and c_{ps} are the specific heats for the pore-fluid and solid matrix; ρ_f and ρ_s are the densities of the pore-fluid and solid matrix; λ_{xf} and λ_{xs} are the thermal conductivities of the pore-fluid and solid matrix in the x direction; λ_{yf} and λ_{ys} are the thermal conductivities of the pore-fluid and solid matrix in the y direction, respectively; ϕ is the porosity of the porous medium; V_x and V_y are the Darcy velocities in the x and y directions; T is the temperature of the porous medium.

Using the Galerkin weighted residual method (Zienkiewicz 1977; Rao 1989), Eq. (7.90) can be discretized into a set of algebraic equations as follows:

$$[\hat{G}]\{T\}+[\hat{H}]\{T\}+[\hat{R}]\left\{\frac{\partial T}{\partial t}\right\}=\left\{\hat{f}\right\}, \tag{7.95}$$

where $\{T\}$ is the global nodal temperature vector of the system; $\left\{\hat{f}\right\}$ is the global nodal "load" vector of the system; $[\hat{G}]$, $[\hat{H}]$ and $[\hat{R}]$ are the global property matrices of the system. These global property matrices can be formed by assembling the following element property matrices:

$$[\hat{G}_e]_1 = \iint_A \left(\frac{\lambda_x^m}{(c_p\rho)_m} \frac{\partial[\hat{N}]^T}{\partial x} \frac{\partial[\hat{N}]}{\partial x} + \frac{\lambda_y^m}{(c_p\rho)_m} \frac{\partial[\hat{N}]^T}{\partial y} \frac{\partial[\hat{N}]}{\partial y} \right) dA, \tag{7.96}$$

$$[\hat{H}_e]_1 = \iint_A \left(\alpha V_x [\hat{N}]^T \frac{\partial[\hat{N}]}{\partial x} + \alpha V_y [\hat{N}]^T \frac{\partial[\hat{N}]}{\partial y} \right) dA, \tag{7.97}$$

$$[\hat{R}_e]_1 = \iint_A \left([\hat{N}]^T [\hat{N}] \right) dA, \tag{7.98}$$

where $[\hat{N}]$ is the temperature shape function of the element; $[\hat{N}]^T$ is the transpose of $[\hat{N}]$; A is the area of the element. It needs to be pointed out that Eqs. (7.96), (7.97) and (7.98) hold for both finite elements and transient infinite elements for simulating heat transfer problems in fluid-saturated porous media.

Using the heat transfer functions of transient infinite elements, the temperature shape function matrix of a two-dimensional transient infinite element can be derived. Figure 7.6 shows a two-dimensional four-node transient infinite element, for which the mapping relationship between the global coordinate system and the local one can be expressed as follows:

$$x = \sum_{i=1}^{4} M_i x_i, \tag{7.99}$$

$$y = \sum_{i=1}^{4} M_i y_i, \tag{7.100}$$

where M_i is the mapping function at each node of the element.

$$M_1 = \frac{1}{2}(1-\xi)(1-\eta), \tag{7.101}$$

$$M_2 = \frac{1}{2}(1-\xi)(1+\eta), \tag{7.102}$$

$$M_3 = \frac{1}{2}\xi(1+\eta), \tag{7.103}$$

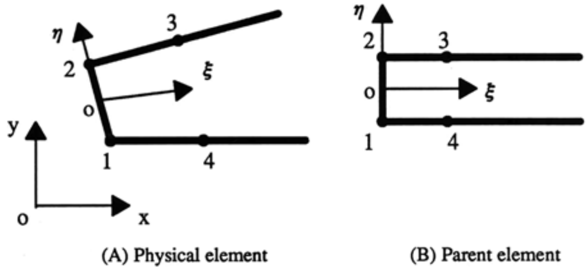

Fig. 7.6 Two-dimensional mapped transient uni-infinite elements

$$M_4 = \frac{1}{2}\xi(1-\eta). \tag{7.104}$$

The temperature field within the two-dimensional transient infinite element shown in Fig. 7.6 can be defined as follows:

$$T = \sum_{i=1}^{2} \hat{N}_i T_i = [\hat{N}] \begin{Bmatrix} T_1 \\ T_2 \end{Bmatrix}, \tag{7.105}$$

where $\hat{N}_1$ and $\hat{N}_2$ are the shape functions of nodes 1 and 2, respectively.

$$\hat{N}_1 = \frac{1}{2} F_{ht}(\xi, t)(1-\eta), \tag{7.106}$$

$$\hat{N}_2 = \frac{1}{2} F_{ht}(\xi, t)(1+\eta). \tag{7.107}$$

Since the number of nodes used for defining the shape of the two-dimensional transient infinite element is greater than that used for defining the temperature field of the two-dimensional transient infinite element, the corresponding parent transient infinite element is a superparametric element.

Substituting Eqs. (7.99), (7.100), (7.101) and (7.102) into Eqs. (7.96), (7.97) and (7.98) yields the property matrices of this two-dimensional transient infinite element as follows:

$$[\hat{G}_e]_1 = \int_0^\infty \int_{-1}^1 \left(\frac{\lambda_x^m}{(c_p\rho)_m} \frac{\partial [\hat{N}]^T}{\partial x} \frac{\partial [\hat{N}]}{\partial x} + \frac{\lambda_y^m}{(c_p\rho)_m} \frac{\partial [\hat{N}]^T}{\partial y} \frac{\partial [\hat{N}]}{\partial y} \right) |J|\, d\eta d\xi, \tag{7.108}$$

$$[\hat{H}_e]_1 = \int_0^\infty \int_{-1}^1 \left(\alpha V_x [\hat{N}]^T \frac{\partial [\hat{N}]}{\partial x} + \alpha V_y [\hat{N}]^T \frac{\partial [\hat{N}]}{\partial y} \right) |J|\, d\eta d\xi, \tag{7.109}$$

$$[\hat{R}_e]_1 = \int_0^\infty \int_{-1}^1 \left([\hat{N}]^T [\hat{N}] \right) |J|\, d\eta d\xi, \tag{7.110}$$

where $|J|$ is the Jacobian determinant of the two-dimensional transient infinite element.

By using the variable substitution technique and letting $\xi = (1+\beta)/(1-\beta)$, Eqs. (7.108), (7.109) and (7.110) can be rewritten into the following forms:

$$[\hat{G}_e]_1 = \int_{-1}^1 \int_{-1}^1 \left(\frac{\lambda_x^m}{(c_p\rho)_m} \frac{\partial [\hat{N}]^T}{\partial x} \frac{\partial [\hat{N}]}{\partial x} + \frac{\lambda_y^m}{(c_p\rho)_m} \frac{\partial [\hat{N}]^T}{\partial y} \frac{\partial [\hat{N}]}{\partial y} \right) \frac{2}{(\beta-1)^2} |J|\, d\eta d\beta, \tag{7.111}$$

$$[\hat{H}_e]_1 = \int_{-1}^1 \int_{-1}^1 \left(\alpha V_x [\hat{N}]^T \frac{\partial [\hat{N}]}{\partial x} + \alpha V_y [\hat{N}]^T \frac{\partial [\hat{N}]}{\partial y} \right) \frac{2}{(\beta-1)^2} |J|\, d\eta d\beta, \tag{7.112}$$

$$[\hat{R}_e]_1 = \int_{-1}^{1}\int_{-1}^{1}\left([\hat{N}]^T[\hat{N}]\right)\frac{2}{(\beta-1)^2}\,|J|\,d\eta d\beta. \tag{7.113}$$

Equations (7.111), (7.112) and (7.113) indicate that the property matrices of the two-dimensional transient infinite element can be evaluated using the Gauss–Legendre integration scheme.

It is noted that under certain situations, a two-dimensional three-node transient bi-infinite element, as shown in Fig. 7.7, can be useful for the numerical analysis. Similarly, the mapping relationship of this two-dimensional three-node transient bi-infinite element can be defined as follows:

$$x = \sum_{i=1}^{3} M_i x_i, \tag{7.114}$$

$$y = \sum_{i=1}^{3} M_i y_i, \tag{7.115}$$

where M_i is the mapping function at each node of the two-dimensional three-node transient bi-infinite element.

$$M_1 = (1-\xi)(1-\eta), \tag{7.116}$$

$$M_2 = \frac{1}{2}\xi(1+\eta), \tag{7.117}$$

$$M_3 = \frac{1}{2}(1+\xi)\eta. \tag{7.118}$$

The temperature shape function for this two-dimensional three-node transient bi-infinite element can be expressed as follows:

$$[\hat{N}] = [\hat{N}_1] = [F_{ht}(\xi,t)F_{ht}(\eta,t)]. \tag{7.119}$$

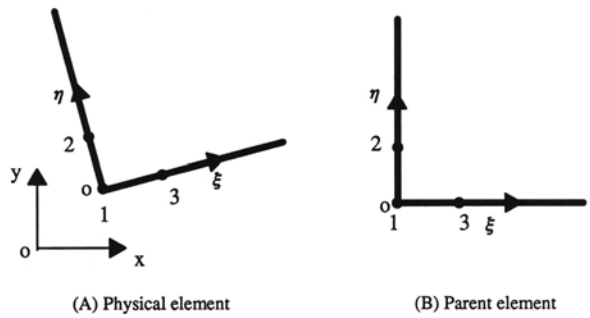

Fig. 7.7 Two-dimensional mapped transient bi-infinite elements

Finally, the property matrices of the two-dimensional three-node transient bi-infinite element can be derived.

$$[\hat{G}_e]_2 = \int_{-1}^{1}\int_{-1}^{1}\left(\frac{\lambda_x^m}{(c_p\rho)_m}\frac{\partial[\hat{N}]^T}{\partial x}\frac{\partial[\hat{N}]}{\partial x} + \frac{\lambda_y^m}{(c_p\rho)_m}\frac{\partial[\hat{N}]^T}{\partial y}\frac{\partial[\hat{N}]}{\partial y}\right) \times \frac{4}{(\beta-1)^2(\gamma-1)^2}|J|\,d\gamma d\beta, \tag{7.120}$$

$$[\hat{H}_e]_2 = \int_{-1}^{1}\int_{-1}^{1}\left(\alpha V_x[\hat{N}]^T\frac{\partial[\hat{N}]}{\partial x} + \alpha V_y[\hat{N}]^T\frac{\partial[\hat{N}]}{\partial y}\right)\frac{4}{(\beta-1)^2(\gamma-1)^2}|J|\,d\gamma d\beta, \tag{7.121}$$

$$[\hat{R}_e]_2 = \int_{-1}^{1}\int_{-1}^{1}\left([\hat{N}]^T[\hat{N}]\right)\frac{2}{(\beta-1)^2(\gamma-1)^2}|J|\,d\gamma d\beta, \tag{7.122}$$

7.3 Verification of Transient Infinite Elements for Simulating Pore-Fluid Flow and Heat Transfer Problems in Fluid-Saturated Porous Media of Infinite Domains

7.3.1 Verification of Transient Infinite Elements for Simulating a Pore-Fluid Flow Problem in the Fluid-Saturated Porous Medium of an Infinite Domain

The correctness and usefulness of the proposed transient infinite element theory can be verified by some simple but critical problems, for which the exact analytical solutions are already available. To examine the two-dimensional behaviour of the proposed transient infinite element theory, a fundamental problem with a given hydraulic head at the centre of a horizontal infinite plane is considered in this subsection. Figure 7.8 shows the discretized model of this problem, where the origin of the global coordinate system is subjected to a given point hydraulic head with the value of 10 m (i.e. $h_0 = 10\,\text{m}$) at $t = 0$. The near field of the system, which is chosen as $80 \times 80\,\text{m}$, has been simulated by two-dimensional four-node square finite elements, while the far field is simulated by eight categories of two-dimensional transient infinite elements as proposed in Sect. 7.1. The following parameters are used in the numerical analysis: the specific storage of the porous medium is $10^{-6}(1/\text{m})$; the hydraulic conductivities are $2 \times 10^{-6}\text{m/day}$ in the x and y directions; the time step used in the computation is 10 days.

Figure 7.9 shows the comparison between the current numerical solutions and the analytical ones (Lardner and Song 1991). In this figure, the dimensionless hydraulic head distributions in the near field of the first quadrant of the global coordinate system, namely in the region of $40\,\text{m} \geq x \geq 0$ and $40\,\text{m} \geq y \geq 0$, have been

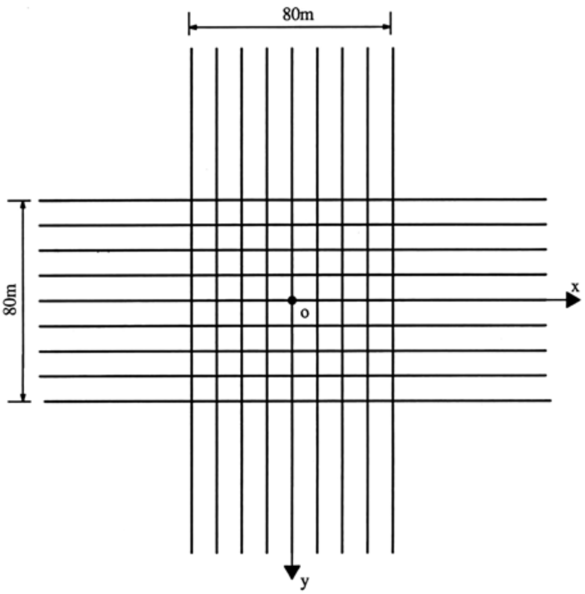

Fig. 7.8 Computational model for simulating a transient pore-fluid flow problem in the fluid-saturated porous medium of an infinite domain: the near field is simulated using 64 finite elements, while the far field is simulated using 36 transient infinite elements.

displayed at three different time instants. From the numerical solutions shown in Fig. 7.9, it can be observed that excellent coincidence exists between the current numerical results with the analytical solutions, even though the near field simulated by finite elements is very small. This demonstrates that the proposed transient infinite element theory is very useful for the numerical simulation of transient pore-fluid flow problems in fluid-saturated porous media of infinite domains.

7.3.2 Verification of Transient Infinite Elements for Simulating a Heat Transfer Problem in the Fluid-Saturated Porous Medium of an Infinite Domain

In this case, a fundamental problem with a given point temperature at the centre of a horizontal infinite plane is considered. As shown in Fig. 7.10, the origin of the global coordinate system is subjected to a unit point temperature, $T_0 = \delta(t)\delta(x)\delta(y)$. The computation domain is divided into an interior domain that is referred to as the near field of the system and an exterior domain that is considered as the far field of the system. The region of the near field is chosen as $80 \times 80\,\text{m}$ and simulated by 64 two-dimensional finite elements, while the far field is simulated by 32 two-dimensional transient infinite elements and 4 two-dimensional transient bi-infinite elements as proposed in Sect. 7.2. Supposing the porous medium is made of clay, the following parameters are used in the numerical analysis: the equivalent product of specific heat and density (i.e. $(c_p\rho)_m$) of the porous medium is $396\,\text{kcal}/(\text{m}^3\cdot{}^\circ\text{C})$; the

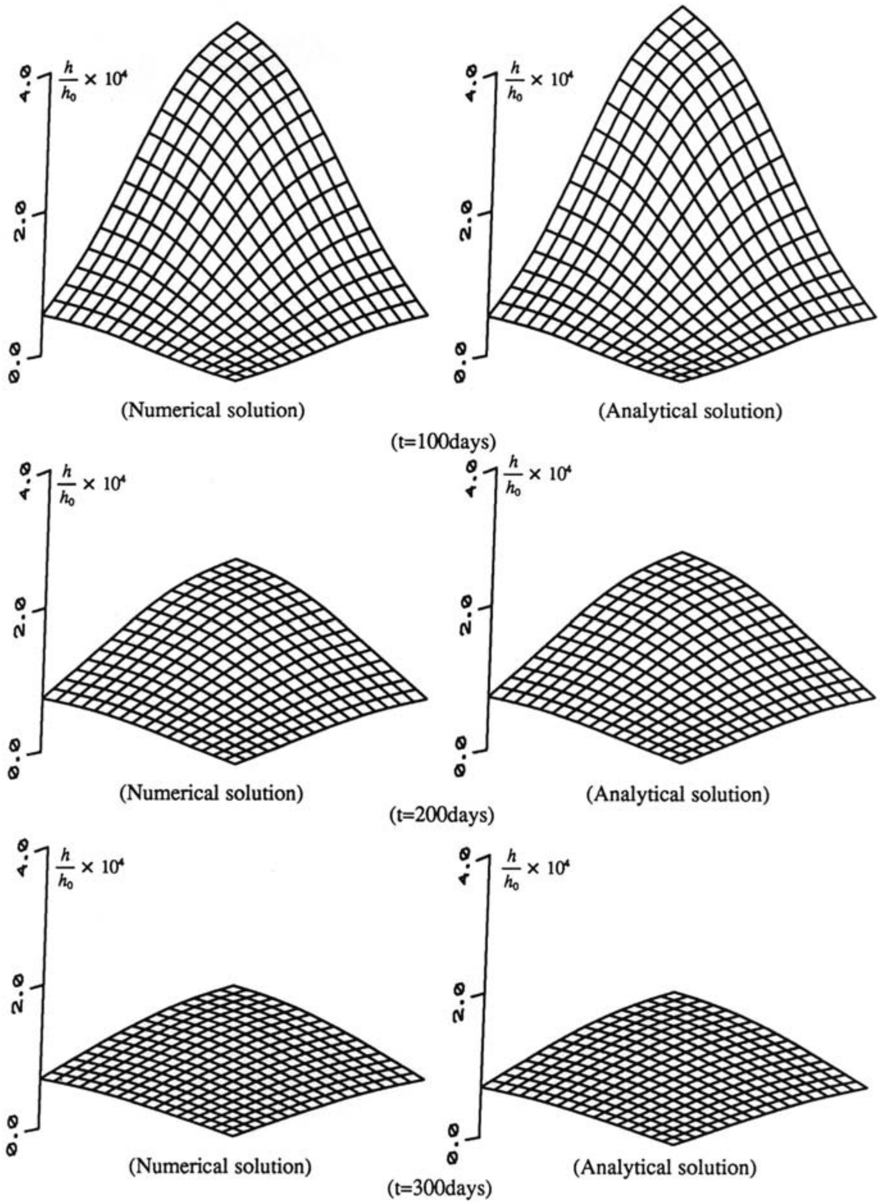

Fig. 7.9 Comparisons of numerical simulation results with analytical solutions for the transient pore-fluid flow problem

thermal conductivity coefficients of the porous medium are 25.92 kcal/(m · day · ° C) in both the x and y directions. It is assumed that no pore-fluid flow occurs in the porous medium so that $V_x = 0$ and $V_y = 0$. The time step used in the computation is 300 days.

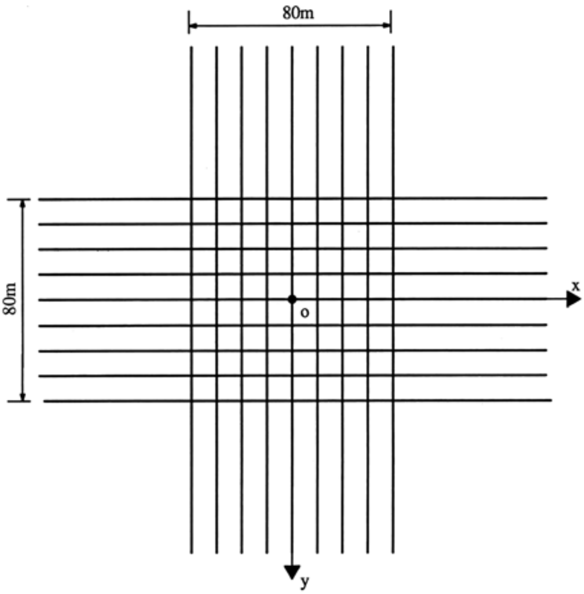

Fig. 7.10 The verification example for simulating a transient heat transfer problem in the fluid-saturated porous medium of an infinite domain: the near field is simulated using 64 finite elements, while the far field is simulated using 36 transient infinite elements

Figure 7.11 shows the comparison between the current numerical solutions and the previous analytical ones (Lardner and Song 1991). It is clear from these results that although the maximum time to be considered in the numerical analysis is 15000 days, there is no evidence that the temperature at any point is approaching a constant value. This indicates that the time-dependent effect is important for most transient heat transfer problems in fluid-saturated porous media. As expected, the symmetrical distribution of the temperature has been obtained at symmetrical locations of the system. For example, three locations, namely $x = 20$ m, $y = 0$ and $x = 0$, $y = 20$ m as well as $x =– 20$ m, $y = 0$, have the same temperature due to their symmetrical characteristics. It is also observed that even though the near field simulated by finite elements is very small, there exists excellent agreement between the current numerical results and the previous analytical solutions, except for a little oscillation at an early time. This oscillation is due to the rapid variation of temperature within a very short time and can be eliminated using a smaller time step in the computation. Therefore, it has demonstrated that the proposed transient infinite element theory is very useful for the numerical simulation of transient heat transfer problems in fluid-saturated porous media of infinite domains.

In summary, transient infinite element theory has been presented for simulating transient pore-fluid flow and heat transfer problems in fluid-saturated orthotropic porous media of infinite domains. Two different ways are used to derive the property matrices of transient infinite elements. In the first way, more different kinds of parent infinite elements with different shapes are used in the process of deriving the property matrices of transient infinite elements. In contrast, in the second way, only

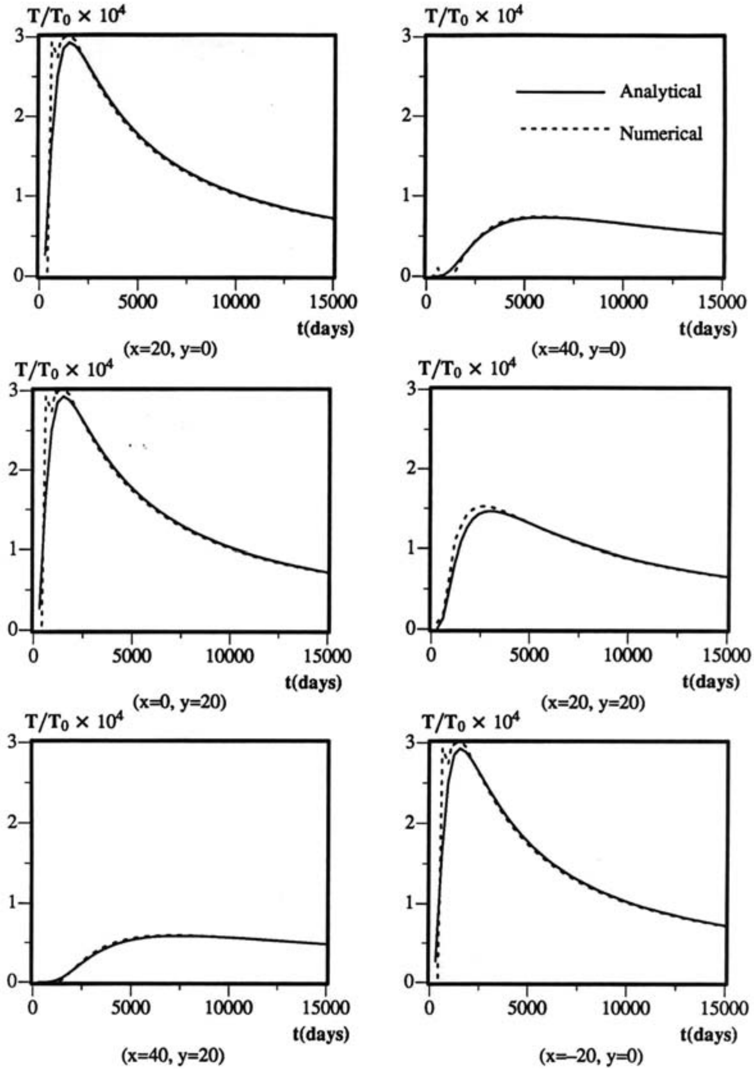

Fig. 7.11 Comparisons of numerical simulation results with analytical solutions for the transient heat transfer problem

two kinds of mapped parent infinite elements are used to derive the property matrices of transient infinite elements. Owing to this significant difference, the property matrices derived using the first way can be expressed in closed forms, but the property matrices derived using the second way need to be evaluated numerically. To demonstrate how to use these two different ways, the first way is used to derive the property matrices of two-dimensional transient infinite elements that can be employed to simulate transient pore-fluid flow problems in fluid-saturated orthotropic porous media of infinite domains, while the second way is employed to derive the property matrices of two-dimensional transient infinite elements, which can be used for simulating transient heat transfer problems in fluid-saturated orthotropic porous media of infinite domains.

Although the transient infinite element theory is presented on the basis of two-dimensional problems, it can be straightforwardly extended to the simulation of three-dimensional transient pore-fluid flow and heat transfer problems in fluid-saturated orthotropic porous media of infinite domains. In addition, the present transient infinite element theory can also be extended to the simulation of coupled problems of transient pore-fluid flow, mass transport and heat transfer in fluid-saturated orthotropic porous media of infinite extent. However, for a porous medium of general anisotropy, the formulation of two- and three-dimensional transient infinite elements remains unavailable so that future research is needed in this respect.